ORIGINAL RESEARCH

Spontaneous Lung Fibrosis Resolution Reveals Novel Antifibrotic Regulators

Qi Tan[1], Patrick A. Link[1], Jeffrey A. Meridew[1], Tho X. Pham[2], Nunzia Caporarello[1], Giovanni Ligresti[1,2], and Daniel J. Tschumperlin[1]

[1]Department of Physiology and Biomedical Engineering, Mayo Clinic, Rochester, Minnesota; and [2]Department of Medicine, Boston University School of Medicine, Boston, Massachusetts

Abstract

Fibroblast activation is transient in successful wound repair but persistent in fibrotic pathologies. Understanding fibroblast deactivation during successful wound healing may provide new approaches to therapeutically reverse fibroblast activation. To characterize the gene programs that accompany fibroblast activation and reversal during lung fibrosis resolution, we used RNA sequencing analysis of flow sorted Col1α1-GFP–positive and CD45-, CD31-, and CD326-negative cells isolated from the lungs of young mice exposed to bleomycin. We compared fibroblasts isolated from control mice with those isolated at Days 14 and 30 after bleomycin exposure, representing the peak of extracellular matrix deposition and an early stage of fibrosis resolution, respectively. Bleomycin exposure dramatically altered fibroblast gene programs at Day 14. Principal component and differential gene expression analyses demonstrated the predominant reversal of these trends at Day 30. Upstream regulator and pathway analyses of reversing "resolution" genes identified novel candidate antifibrotic genes and pathways. Two genes from these analyses that were decreased in expression at Day 14 and reversed at Day 30, Aldh2 and Nr3c1, were selected for further analysis. Enhancement of endogenous expression of either gene by CRISPR activation in cultured human idiopathic pulmonary fibrosis fibroblasts was sufficient to reduce profibrotic gene expression, fibronectin deposition, and collagen gel compaction, consistent with roles for these genes in fibroblast deactivation. This combination of RNA sequencing analysis of freshly sorted fibroblasts and hypothesis testing in cultured idiopathic pulmonary fibrosis fibroblasts offers a path toward identification of novel regulators of lung fibroblast deactivation, with potential relevance to understanding fibrosis resolution and its failure in human disease.

Keywords: RNA-seq; CRISPR activation; Aldh2; Nr3c1; fibrosis resolution

Clinical Relevance

The current study seeks to explore the homeostatic and fibrosis-resolving roles of novel genes in lung fibroblasts and to develop a new regenerative therapeutic strategy to treat lung fibrosis using non–genome-editing CRISPR gene activation to promote fibrosis resolution. The outcomes from proposed studies are expected to have an important positive impact on human chronic lung diseases because the identification and application of novel antifibrotic regulators will help to overcome current limitations of treating pulmonary fibrosis in human patients.

(Received in original form August 29, 2020; accepted in final form December 18, 2020)

Supported by National Institutes of Health grants HL153026 (Q.T.), HL142596 (G.L.), HL 105355 (P.A.L.), HL092961 (D.J.T.), and HL133320 (D.J.T.).

Author Contributions: Q.T.: funding acquisition, conceptualization, data acquisition and analysis, methodology, and the manuscript writing and editing. P.A.L.: methodology and data analysis, and the manuscript editing. J.A.M.: data acquisition. T.X.P.: data acquisition, data analysis, and the manuscript editing. N.C.: data acquisition and the manuscript editing. G.L.: conceptualization and the manuscript editing. D.J.T.: funding acquisition, conceptualization, data analysis, supervision, and the manuscript writing and editing.

Correspondence and requests for reprints should be addressed to Qi Tan, Ph.D., Assistant Professor of Biomedical Engineering, Department of Physiology and Biomedical Engineering, Mayo Clinic College of Medicine and Science, 200 First Street SW, Rochester, MN 55905. E-mail: tan.qi@mayo.edu.

This article has a related editorial.

This article has a data supplement, which is accessible from this issue's table of contents at www.atsjournals.org.

Am J Respir Cell Mol Biol Vol 64, Iss 4, pp 453–464, Apr 2021

Originally Published in Press as DOI: 10.1165/rcmb.2020-0396OC on January 25, 2021
Internet address: www.atsjournals.org

Fibroblasts are central regulators of extracellular matrix deposition and maintenance. In normal wound healing, fibroblasts become transiently activated to aid in the formation and contraction of a provisional extracellular matrix (ECM) scaffold. In fibrotic pathologies, fibroblasts are persistently activated, leading to excessive and disorganized fibrotic scarring. In normal healing, repair is accompanied by resolution and resorption of excess ECM, accompanied by fibroblast deactivation or apoptosis of activated fibroblasts (1). Bleomycin injury is widely used to study fibroblast activation and fibrosis in the lung (2). However, in young mice, bleomycin-induced ECM deposition spontaneously reverses (3, 4). Our understanding of the process and mechanisms controlling lung fibrosis resolution lags far behind our understanding of fibroblast activation (5), and very little is known about the state of lung fibroblasts during this resolution process. Understanding whether and how fibroblasts become deactivated in normal lung healing could lead to novel approaches for therapeutic intervention in fibrotic pathologies such as idiopathic pulmonary fibrosis (IPF). A similar approach to the study of liver fibrosis has demonstrated the remarkable degree to which hepatic stellate cells exhibit deactivation during fibrosis resolution (6–8). Here, we set out to test a similar concept in lung fibrosis, using a Col1α1-GFP marker and negative selection to sort fibroblasts from the lung and comparing time points after bleomycin injury associated with peak fibrogenic activation (14 d after bleomycin) and an early stage of fibrosis resolution (30 d after bleomycin). We employed a CRISPR activation technique to test whether enhancing the expression of candidate genes repressed during fibrosis and elevated during lung fibrosis resolution exerts antifibrotic effects in lung fibroblasts isolated and cultured from individuals with diagnosed IPF. We found that fibroblasts as a population exhibit a remarkable plasticity in undergoing transient activation at Day 14 (D14) after bleomycin exposure that largely reverses by Day 30 (D30) after bleomycin exposure, a time at which fibrosis resolution and repair is only beginning. Moreover, two genes identified as transiently repressed during fibrosis and restored at D30, *Aldh2* (aldehyde dehydrogenase 2) and *Nr3c1* (nuclear receptor subfamily 3 group C member 1), exerted antifibrotic effects on fibroblast gene expression, fibronectin deposition, and collagen gel compaction when their expression was enhanced in IPF fibroblasts. Together, these findings demonstrate the utility of studying fibrosis resolution pathways in the bleomycin model and suggest that resolution genes reexpressed in fibroblasts during lung repair may actively participate in the termination of fibroblast activation and tissue fibrosis.

Methods

Bleomycin Administration to Mice

All experiments were performed in accordance with the Mayo Clinic Institutional Animal Care and Use Committee. Col1α1-GFP transgenic mice were kindly provided by Dr. Derek Radisky and generated as previously described (9). Eight-week-old mice were anesthetized with 90–120 mg/kg ketamine and 10 mg/kg xylazine. Mice were exposed to 1.2 U/kg bleomycin (APP Pharmaceutical) or PBS delivered intratracheally using a MicroSprayer (Penn-Century).

Flow Cytometry and RNA Sequencing Analysis

Mice were killed on D14 or D30 after bleomycin treatment (3) for isolation of fibroblasts during active fibrosis and at early stages of fibrosis resolution. Col1α1-GFP$^+$ fibroblasts were freshly sorted into the lysis buffer from RNeasy Micro Kit (QIAGEN), and RNA was isolated and purified by RNeasy Micro Kit (QIAGEN) (10). RNA libraries were prepared and sequenced following Illumina's standard protocol using the Illumina cBot and HiSeq 3000 PE Cluster Kit, yielding 33 million to 40 million fragment reads per sample. Differential expression analysis, gene pathway analyses, and upstream analyses were performed.

Cell Culture and CRISPR Activation

Primary human lung fibroblasts isolated by explant culture from the lungs of subjects with diagnosed IPF who underwent lung transplantation or donors whose organs were rejected for transplantation (non-IPF control subjects) were kindly provided by Peter Bitterman and Craig Henke at the University of Minnesota under a protocol approved by the University of Minnesota Institutional Review Board. CRISPR-mediated gene activation was carried using a catalytically dead Cas9 (dCas9) fused to their activator VP64-p65-Rta (VPR) and combined with short guide RNA (gRNA) to direct the dCas9-VPR to specific target gene, as in our previous publication (11).

Statistical Analysis

Data shown are expressed as mean ± SD. We performed statistical comparisons using Mann-Whitney test for groups of two or one-way ANOVA for groups larger than two. We used GraphPad Prism 8 (GraphPad Software) for all statistical analyses. We determined *P* values of less than 0.05 to be statistically significant. We performed all the *in vitro* experiments three times, and representative data are shown.

For additional details on the Methods, *see* the data supplement.

Results

RNA Sequencing Analysis Reveals Dramatic but Transient Changes in Fibroblast Transcriptomic State after Bleomycin Exposure

To evaluate changes in gene expression of lung fibroblasts during fibrosis initiation and resolution after bleomycin administration, we employed a Col1α1-GFP transgenic mouse combined with flow sorting to isolate Col1α1-GFP$^+$ fibroblasts. FACS and hydroxyproline analyses from our previous study using this same mouse strain and cell sorting strategy (3) identified D14 as the approximate peak of fibrosis and fibroblast activation, with reversal of both processes in their early stages at D30. Therefore, we chose D14 and D30 as representing fibrotic and early fibrosis resolution stages. Briefly, bleomycin was intratracheally delivered to the lungs of mice at Day 0, and Col1α1-GFP$^+$ fibroblasts were sorted at D14 and D30 after bleomycin exposure and, at the same times from sham controls (Figure 1A), followed by RNA isolation and RNA sequencing (RNA-seq) analysis.

Principal components analysis was first used to visualize the overall trend in transcript changes after bleomycin exposure. This analysis revealed that the sham group, D14 post-bleomycin group, and D30 post-bleomycin group formed distinct clusters (Figure 1B). Notably, the sham group and D30 bleomycin group shared a similar position on the horizontal axis, representing principal component 1,

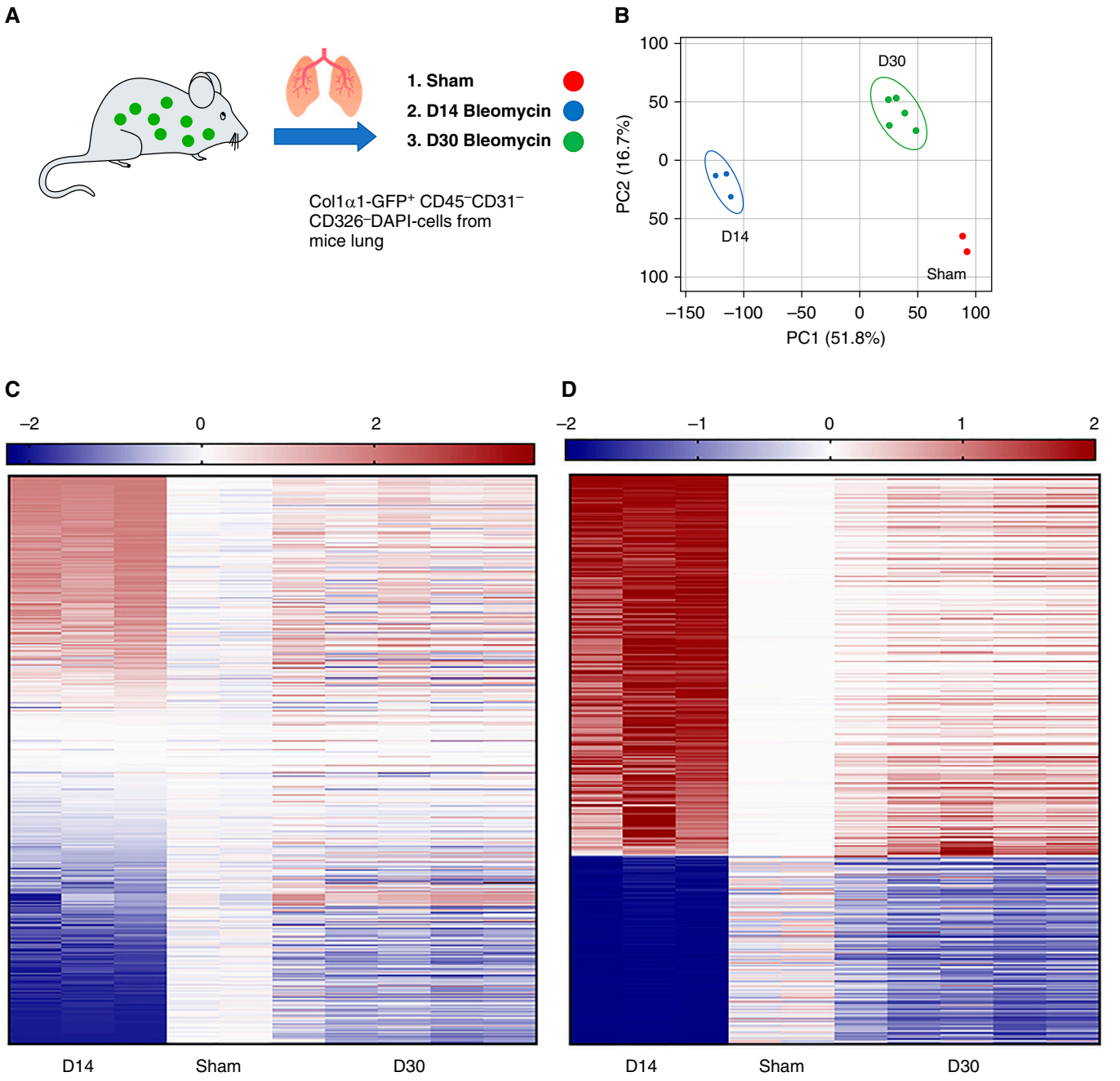

Figure 1. Principal component analysis and gene expression heatmaps reveal spontaneous reversal of bleomycin-induced fibroblast activation. (*A*) Col1α1-GFP^{+} lung fibroblasts were sorted for RNA sequencing (RNA-seq) analysis (sham, $N = 2$; Day 14 [D14] bleomycin, $N = 3$; Day 30 [D30] bleomycin, $N = 5$). (*B*) Principal components analysis of RNA-seq data (top 12,000 expressed genes from sham group) from sham group, D14 bleomycin group, and D30 bleomycin group. (*C*) Heatmap shows top 1,000 expressed genes from sham among three groups. (*D*) Heatmap shows differentially expressed genes from sham and D14 bleomycin among three groups. Col1α1 = collagen type 1 alpha 1; PC1 = principal component 1; PC2 = principal component 2.

which captures the largest fraction of the sample variance. In contrast, the D14 group was distant from this shared principal component 1 value, demonstrating that fibroblasts isolated at D14 diverged from sham fibroblasts and were transcriptionally distinct from those isolated at D30 after bleomycin (Figure 1B). Figure 1C shows a heatmap of the top 1,000 expressed genes in the sham group and their changes in expression in the D14 and D30 groups. The large majority of genes shown in red and blue, particularly at D14, emphasize the degree to which bleomycin dramatically alters the transcriptional state of lung fibroblasts. Similar to the principal components analysis, this heatmap illustrates the pronounced, but relatively transient, transcriptomic fingerprint of bleomycin-induced fibroblast activation that is present at D14 but spontaneously

weakened by D30 (Figure 1C). Figure 1D focuses on the genes differentially expressed [false discovery rate (FDR) < 0.05; log2(fold change) >1 or <-1] between sham and D14 bleomycin groups. This analysis further highlights the dramatic transcriptional effects observed at D14 after bleomycin, with 1,897 differentially repressed genes and 2,227 differentially elevated genes compared with the sham group (Figure 1D and Table E1 in the data supplement). Once again, the heatmaps demonstrate the reversibility of the bleomycin-induced changes in fibroblast gene expression observed between D14 and D30 after bleomycin, with widespread reversion of expression back toward sham concentrations. Together, these analyses highlight that extent to which lung fibroblast transcriptional changes after bleomycin exposure in young mice are spontaneously reversed on a relatively rapid time scale.

Major Profibrotic and Antifibrotic Genes and Pathways Are Detected at D14 after Bleomycin

We next focused on characterizing individual genes and key pathways differentially expressed in fibroblasts at D14 after bleomycin as a validation of our overall approach. As stated above, we identified 2,227 differentially elevated genes [FDR $<$ 0.05; log2(fold change) $>$ 1] at D14 after bleomycin relative to the sham control group. We observed dramatic increases in expression of key individual genes associated with proliferation (e.g., *Mki67* and *Pcna*), ECM deposition (e.g., *Col1a1*, *Col1a2*, *Fn1*, and *Tnc*), and soluble signaling (e.g., *Cxcr4*, *Ccr5*, *Tgfb1*, and *Tnf*) (Figure 2A). In the opposite direction, we identified 1,897 gene differentially expressed at lower concentrations at D14 after bleomycin compared with the sham control group. Several individual genes previously or potentially associated with lung fibrosis resolution were noted (Figure 2B), including the gene encoding *Ptgs2* (cyclooxygenase-2) (12), *Ppara* (peroxisome proliferator activated receptor α) (13); extracellular matrix factors, including *Mmp2* (matrix metalloproteinase-2) (14); and the glycoprotein *Dcn* (decorin) (15).

We then applied ingenuity pathway analysis to identify putative upstream regulators of the gene programs differentially expressed at D14. The top enriched upstream regulators confirmed a predominant TGFβ pathway signature (Figure 2C) in fibroblasts activated *in vivo* at D14 and suggested potential roles for IFN-γ, TNF, vascular endothelial growth factor, and IL-6 in fibroblast gene programs activated at D14. TNFα, IFN-γ, and IL-6 are potent proinflammatory cytokines, and their presence as potential upstream regulators suggests that lung fibroblasts may engage in and be engaged by inflammatory signaling similar to that observed in other contexts (16–18). Upstream regulator analysis also suggested loss of FOXO3 and Il-10 pathways known to inhibit cell cycle progression and inflammation (19, 20). IL-10 is an antiinflammatory cytokine with important immunoregulatory functions and is able to inhibit the effects of various profibrotic growth factors and cytokines (21). FoxO3 expression was recently shown to be inhibited by various profibrotic growth factors and cytokines, and FoxO3 deletion leads to enhanced fibroblast proliferation and bleomycin-induced lung fibrosis (19). The entire list is included in Table E2.

We next evaluated the transcriptional trends that emerged at D30 relative to D14 after bleomycin delivery. Interestingly, of transcripts increased at D14, only 0.9% were further elevated at D30 (Figure 2D), whereas 26.5% were statistically unchanged from D14. In contrast, the remaining 72.6% of genes were significantly decreased in expression at D30 relative to D14, with a remarkable 62.1% (1,383 genes) of them no longer differentially expressed relative to the sham group (Table E1). We similarly assessed the fate of the 1,897 D14 differentially repressed genes at D30. Of these, a remarkable 94.9% of genes were significantly increased in expression at D30 relative to D14, with 86.2% (1,635 genes) of them no longer differentially repressed relative to the sham group (Table E1). Only 5.1% of repressed transcripts were statistically unchanged from D14, and none of those genes were further repressed at D30 (Figure 2D).

These results are consistent with a dramatic reversal of the fibroblast transcriptional program that is activated at D14 after bleomycin (Figure 2D). Such spontaneous reversion likely results from the loss of profibrotic signals present after lung injury but is also likely influenced by the activation of genes and pathways that were repressed during the injury and return during successful repair (e.g., FOXO3 and Il10, as noted above). Because much effort has already been focused on the genes and pathways engaged during the fibrotic phase after bleomycin, we turned our efforts to analyzing those genes and pathways repressed at D14 and restored at D30. In particular, we reasoned that genes that exhibit transient repression during fibrosis and increased expression during fibroblast deactivation and fibrotic resolution might exhibit antifibrotic and prorepair activities. Engaging such repair and resolution genes and pathways may offer an attractive alternative to inhibiting the major pathways that drive fibroblast activation.

Novel Candidate Antifibrotic Pathways and Regulators Emerge during the Fibrosis Resolution

In total we identified 3,018 "resolution" genes (Table E1) by combining the genes increased/decreased at D14 and significantly reversed at D30 (Figure 2D). Ingenuity canonical pathway analysis of those pathways repressed at D14 and elevated at D30 is shown in Figure 3A, and the full list is included in the Table E3. These pathways include multiple degradative metabolic pathways as well as fatty acid α-oxidation, glutathione-mediated detoxification, and eicosanoid, calcium, and Wnt Signaling. The degradative metabolic pathways are heavily overlapping in their members and share many similar genes, including members of the ALDH family and UGT family (Figure 3B). Both families are involved in the defense against oxidative stress and detoxification (22). The ALDHs are a superfamily of NADP-dependent enzymes that play a major role in acetaldehyde detoxification (22). ALDH2 has been implicated in cellular antioxidant processes because ALDH2 deficiency increases oxidative stress (23, 24). We reasoned that the coordinated repression during the initial fibrotic phase and elevation during lung repair of these pathways could provide a novel route to understand and promote lung fibroblast deactivation.

As a complementary approach, we sought to identify candidate upstream regulators controlling the observed program of fibroblast gene repression and expression at D14 and D30 after bleomycin exposure (Table E4). For this upstream analysis, we focused on the following three categories: drugs (chemical and biological) (Figure 4A), transcriptional regulators (Figure 4B), and

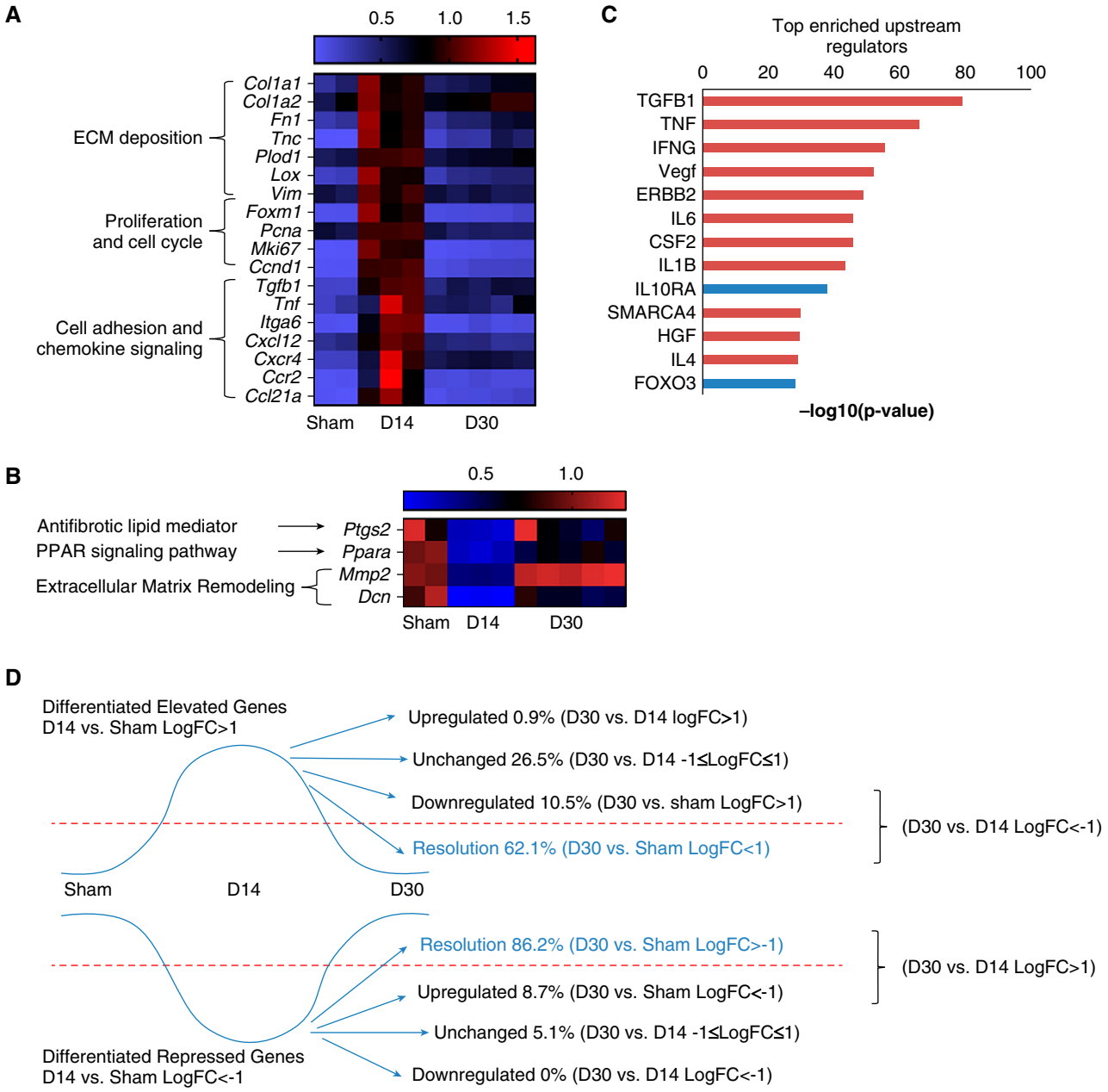

Figure 2. Major profibrotic and antifibrotic genes and pathways detected at D14 after bleomycin. (*A*) Heatmap of representative profibrotic genes among sham, D14 bleomycin, and D30 bleomycin groups. (*B*) Heatmap of representative antifibrotic genes among sham, D14 bleomycin, and D30 bleomycin groups. (*C*) Top enriched upstream regulators at D14 compared with sham. (*D*) The fate of differentially elevated and repressed genes (sham vs. D14 bleomycin) at D30. ECM = extracellular matrix; Fn1 = fibronectin 1; LogFC = log2(fold change); PPAR = peroxisome proliferator-activated receptors.

other regulators (Figure 4C). Using ingenuity pathway analysis, we identified the top upstream factors implicated in the program of genes repressed at D14 relative to sham and increased at D30 relative to D14. Figure 4A suggests multiple drugs that might mimic the spontaneous reversal of fibroblast activation. Promisingly, several of these have previously been identified as antifibrotic in the lung or other experimental fibrosis models. For example, fluticasone propionate (steroids and steroid derivatives) (25), calcitriol (active form of vitamin D) (26), and dexamethasone (steroids) (25) have all been shown to be antifibrotic in previous studies. Other previously implicated regulators include antidiabetic and antifibrotic drugs rosiglitazone (27) and thiazolidinediones (28), the NADPH oxidase (29) inhibitor imipramine blue, and antiaging drug sirolimus (30). Interestingly, several neurally active drugs, including chloropromazine (antipsychotic), haloperidol (antipsychotic) (31), and valproic acid (affecting GABA concentrations), were also identified,

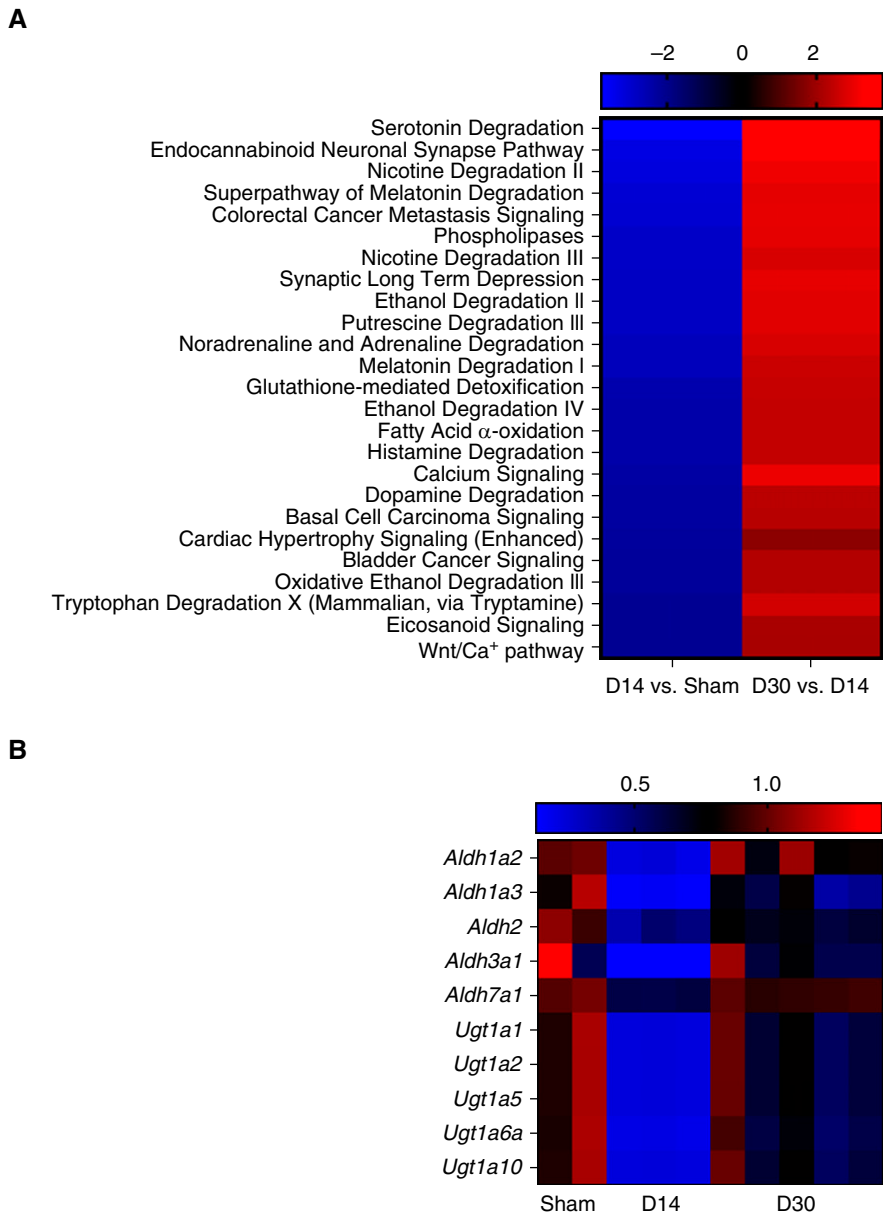

Figure 3. Resolution genes reveal novel antifibrotic pathways during the fibrosis resolution. (*A*) Heatmap of the *z*-scores of pathways repressed at D14 and elevated at D30 from the resolution genes in Figure 2. (*B*) Heatmap of selected genes common to several resolution pathways.

supporting an antifibrotic role of neuronal modulators, which has received some attention (32).

For transcriptional and other upstream regulators (Figure 4B), we identified several that might limit fibrosis by reducing fibroblast cell cycle progression or promoting an adipogenic fate (4), including CEBPA (11), PRDM16 (33), and EBF2 (34). In addition, SIRT1- (35, 36) and FOXO-mediated transcription (19) have previously been shown to exert antifibrotic effects in lung fibrosis. MicroRNA let-7 d was also shown to serve a protective role in preventing lung fibrosis in previous study (37). We also identified multiple G-protein couple receptors, ligand-dependent nuclear receptors, and transmembrane receptors as upstream regulators. These include the prostaglandin E2 receptor 4 (EP4), a receptor for the lung fibroblast inhibitory factor PGE2 (prostaglandin E2) (38).

To narrow our focus and identify specific transcription regulators for further testing, we identified the candidate upstream regulators whose gene expression followed the same pattern of reduced expression at D14 and resolution at D30 (Figures 4D and 4E). This analysis identified eight upstream regulators with coregulated patterns of expression and inferred regulatory function, of which we selected NR3C1 for further analysis. *NR3C1* encodes the glucocorticoid receptor, and the repression of this receptor mediates the glucocorticoid resistance (39) that is often observed during the treatment of chronic inflammatory lung diseases (40). Corticosteroids have previously been observed to reduce myofibroblast accumulation in the airways of mice (41), but their use in treatment of IPF has been contraindicated for several years on the basis of lack of efficacy in a pivotal clinical trial (42). The overall rationale for corticosteroids in IPF was based on their pleiotropic antiinflammatory roles (43), but the direct role of the NR3C1 glucocorticoid nuclear receptor in the regulation of fibroblast fibrogenic activation and deactivation is not well understood. Thus, on the basis of its coordinated repression and reactivation in fibroblasts during fibrosis and resolution, we prioritized NR3C1 for further study.

Single-Cell Sequencing Validates the Lower Expression of Candidate Fibrosis Resolution Genes in IPF

To test whether the proposed antifibrotic genes (*ALDH2* from pathway analysis and *NR3C1* from upstream analysis) are modified in human disease, we queried a publicly available single-cell RNA-seq dataset from Tsukui and colleagues (44) (Figures 5A–5C). We observed that both *ALDH2* and *NR3C1* transcripts were decreased in fibroblasts from IPF lungs compared with control lungs (Figures 5D–5E), with more robust changes in *ALDH2* and more subtle changes in *NR3C1*. As a direct comparison with our analysis of sorted mouse fibroblasts, we also analyzed the single-cell transcript levels from mouse lungs at D14 after bleomycin reported by Tsukui and colleagues (44) (Figures 5F–5H). This analysis confirmed that both *ALDH2* and *NR3C1* transcripts were decreased in fibroblasts as measured by single-cell analysis after bleomycin (Figures 5I–5J). To directly characterize human disease–relevant changes in ALDH2 and GR (glucocorticoid receptor, encoded

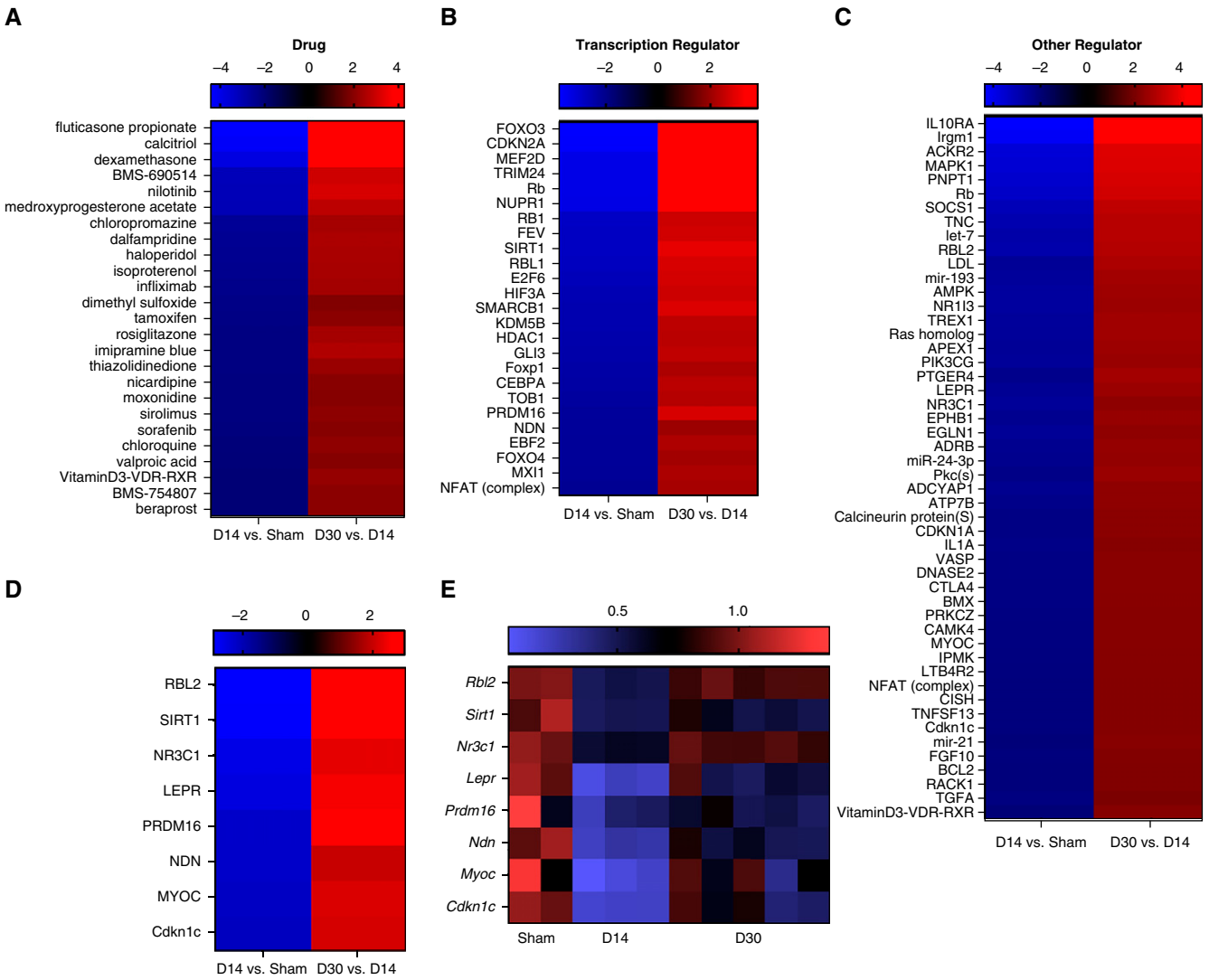

Figure 4. Resolution genes reveal novel upstream regulators during the fibrosis resolution. Heatmaps showing top predicted upstream regulators from (*A*) drug, (*B*) transcription regulators, and (*C*) other regulators as determined by ingenuity pathway analysis from the resolution genes in Figure 2. (*D*) Heatmap of the subset of upstream regulators that show a corresponding change in expression of their nominal gene. (*E*) The relative time pattern of gene expression of the upstream regulators from above (*D*).

by *NR3C1)* protein expression, we compared cultured primary human IPF-derived and healthy control lung fibroblasts. Across donors, we observed lower ALDH2 and GR protein concentrations in IPF fibroblasts compared with fibroblasts from healthy control lung (Figures 5K and 5L), confirming the changes in transcripts levels observed in the single-cell RNA-seq analyses.

CRISPR Activation Validates Antifibrotic Effects of Candidate Fibrosis Resolution Genes

On the basis of our results above, we employed a CRISPR activation approach to test the effects of enhancing specific expression of *ALDH2* and *NR3C1* in human lung fibroblasts from subjects with IPF. We first transfected the CRISPR activation plasmid expressing dCas9-VPR into IPF fibroblasts. After 2 days, synthetic gRNAs targeting the transcriptional start site of each specific gene were then transfected separately into the same cells. After another 2 days, we found that transfection of gRNA significantly increased expression of *ALDH2* and *NR3C1* by quantitative RT-PCR (qRT-PCR) and Western blot (Figures 6A and 6B). Profibrotic gene expression was then evaluated in these cells in the presence or absence of TGFβ1 by qRT-PCR. Both *ALDH2*-gRNA and *NR3C1*-gRNA transfection reduced the expression of profibrotic genes *ACTA2*, *COL1A1*, *FN1*, and *CTGF* (Figure 6C) at baseline as well as in the presence of TGF-β1 treatment. To test the effect of gene activation of *ALDH2* or *NR3C1* on ECM deposition, we used an antibody-based immunostaining method and found gene activation of *ALDH2* or *NR3C1* decreased deposition of fibronectin significantly with TGFβ1 treatment (Figures 6D and 6E). To examine whether *ALDH2* or *NR3C1* activation modulates fibroblast contractile function, we performed collagen gel compaction assays and found that *ALDH2* or *NR3C1* activation diminished TGFβ-mediated fibroblast contraction (Figure 6F). Taken together, these results demonstrate that

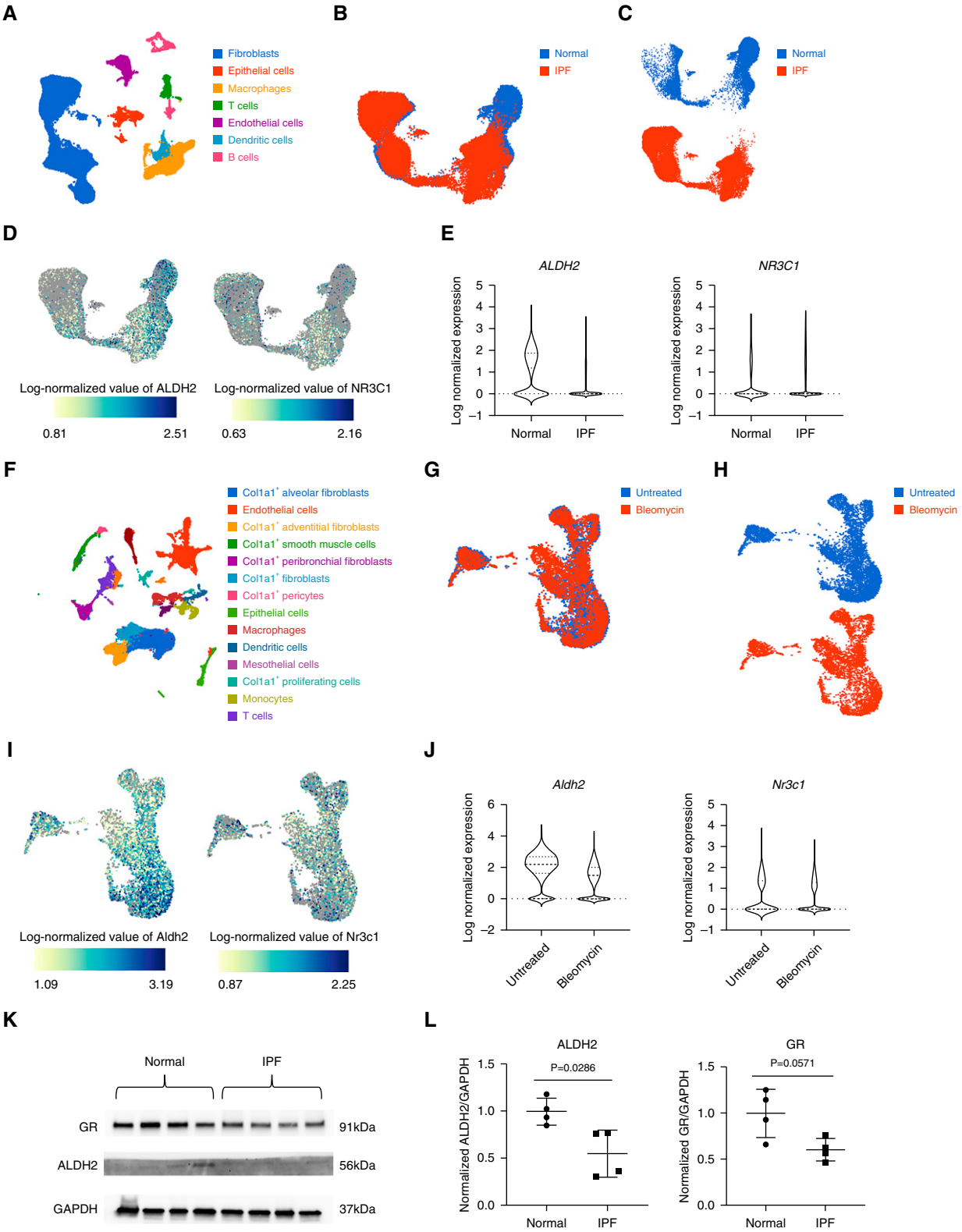

Figure 5. Single-cell sequencing validates the lower expression of candidate fibrosis resolution genes in idiopathic pulmonary fibrosis (IPF). (*A*) UMAP plot of all human cells from the single-cell RNA-seq dataset of Tsukui and colleagues (*B*) UMAP plot of the reclustered fibroblast population. (*C*) UMAP plot of reclustered fibroblast population stratified by sample type. (*D*) Expression of *ALDH2* and *NR3C1* overlaid on UMAP plots. (*E*) Violin plot of *ALDH2* and *NR3C1* expression in normal and IPF fibroblasts. (*F*) UMAP plot of all mouse lung cells from the single-cell RNA-seq dataset of Tsukui and colleagues (*G*) UMAP plot of the reclustered fibroblast populations comprising of Col1a1^{+} alveolar, adventitial, and peribronchial fibroblasts and Col1a1^{+} fibroblasts.

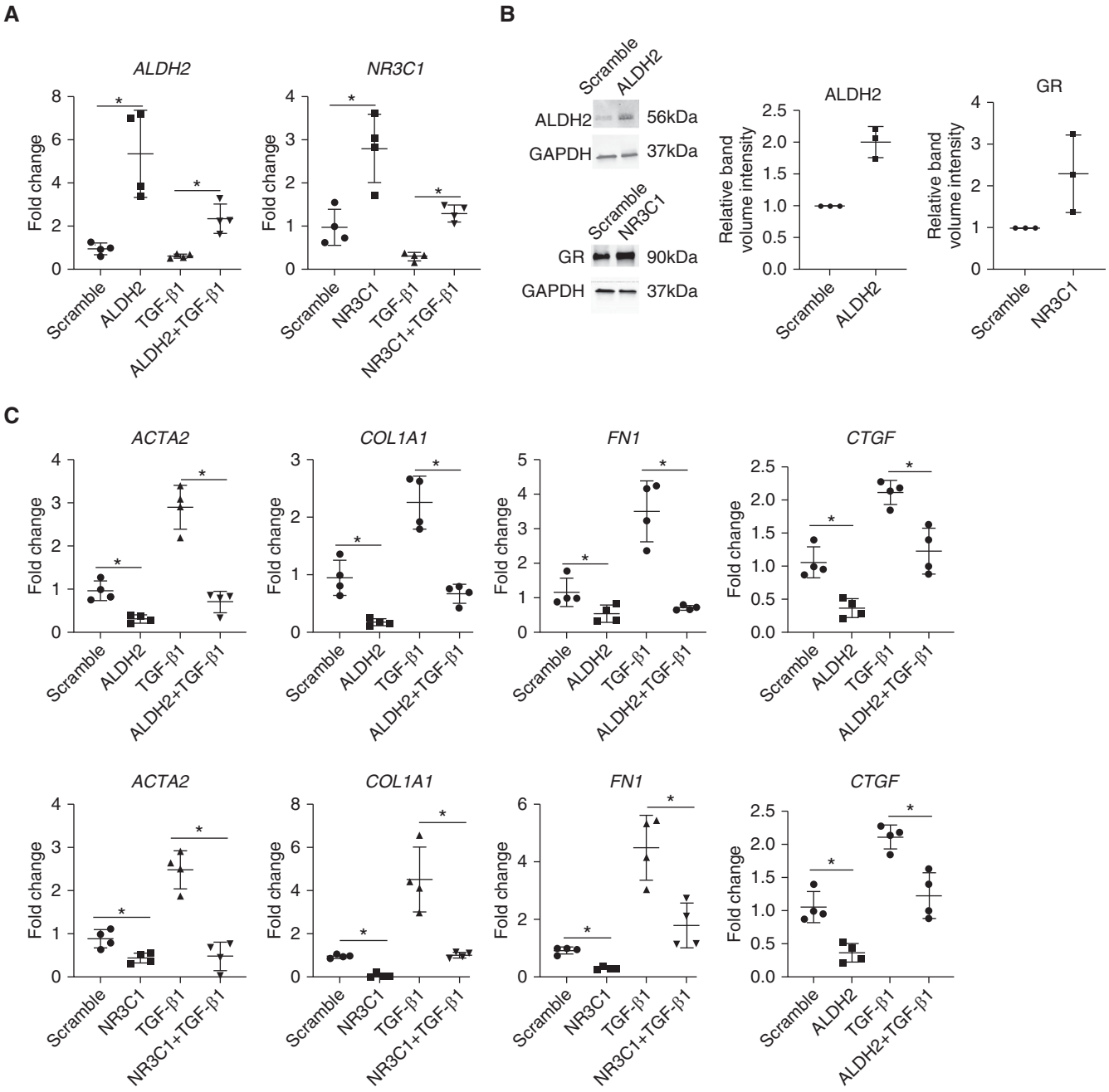

Figure 6. CRISPR activation of candidate resolution genes exerts antifibrotic effects on human lung fibroblasts. (*A*) Quantitative RT-PCR (qRT-PCR) analysis of *ALDH2* and *NR3C1* expression in the dead Cas9 (dCAS9)–expressing IPF fibroblasts with nontargeting gRNA or *ALDH2/NR3C1* gRNA. (*B*) Western blot analysis of ALDH2 and NR3C1 expression in the dCAS9-expressing IPF fibroblasts with nontargeting guide (gRNA) or *ALDH2/NR3C1* gRNA. (*C*) qRT-PCR analysis of profibrotic gene expression in the dCAS9-expressing IPF fibroblasts with nontargeting gRNA or *ALDH2/NR3C1* gRNA. (*D*) Immunostaining showing deposition of fibronectin in the dCAS9-expressing IPF fibroblasts with nontargeting gRNA or *ALDH2/NR3C1* gRNA and (*E*) their quantification. (*F*) Collagen gel compaction assay showing the percentage of diameter decrease in collagen gels by embedded dCAS9-expressing IPF fibroblasts with nontargeting gRNA or *ALDH2/NR3C1* gRNA. (*G*) Schematic showing the proposed role of profibrotic and antifibrotic factors in the balance between fibroblast quiescence and activation. $^{*}P < 0.05$, $^{**}P < 0.01$, $^{***}P < 0.001$, and $^{****}P < 0.0001$. Scale bars, 100 μm. CTGF = connective tissue growth factor; ns = not significant; TGF-β1 = transforming growth factor β 1.

Figure 5. (*Continued*). (*H*) UMAP plot of reclustered fibroblast populations stratified by sample type. (*I*) Expression of *Aldh2* and *Nr3c1* overlaid on UMAP plots. (*J*) Violin plot of *Aldh2* and *Nr3c1* expression in fibroblasts of control or bleomycin-treated mice. (*K*) Western blot analysis showing ALDH2 and GR protein expression in control lung fibroblasts ($N = 4$) and IPF-derived fibroblasts ($N = 4$) together with quantification (*L*). ALDH2/Aldh2 = aldehyde dehydrogenase 2; GR = glucocorticoid receptor, encoded by NR3C1 protein; NR3C1/Nr3c1 = nuclear receptor subfamily 3 group C member 1; UMAP = uniform manifold approximation and projection.

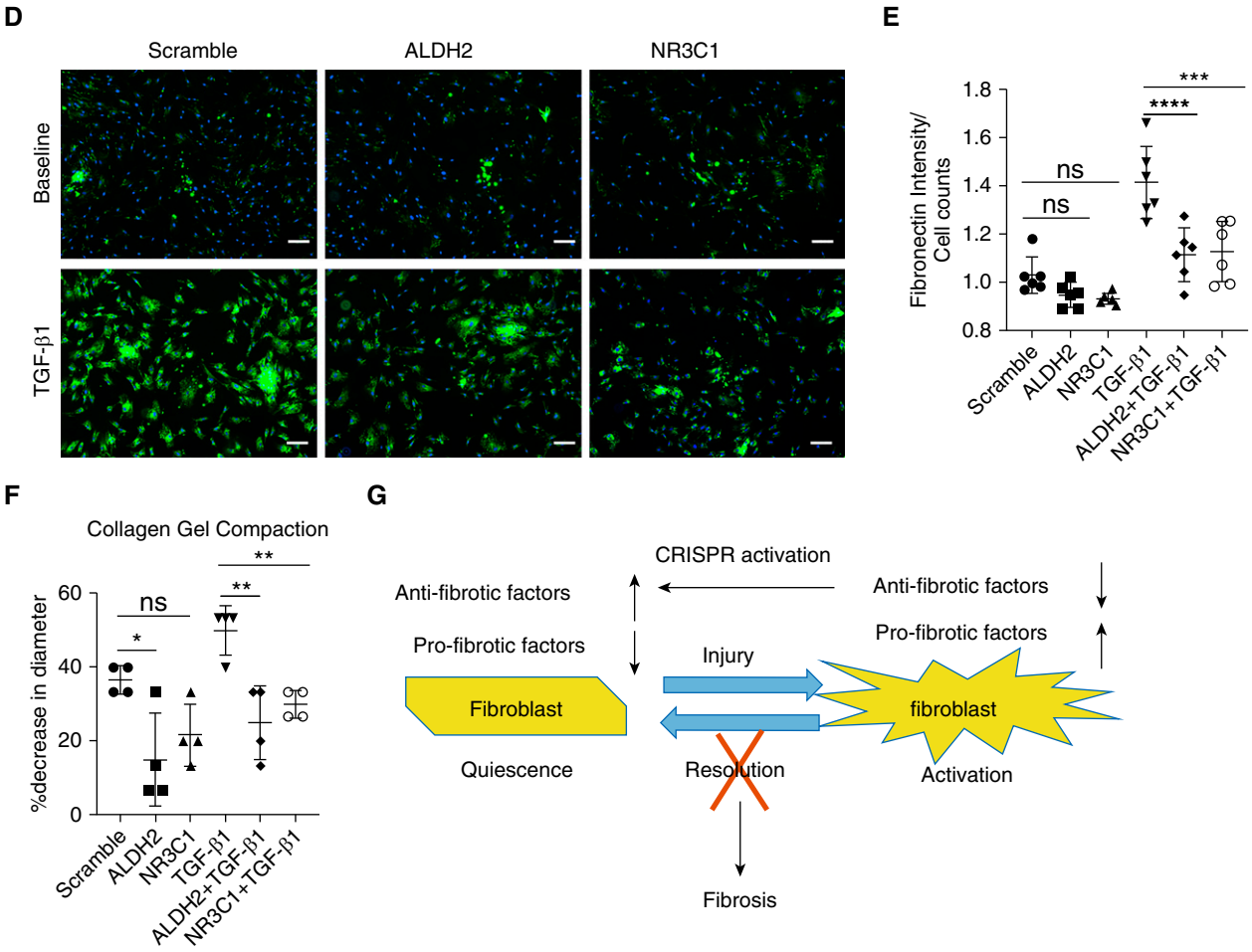

Figure 6. (*Continued*).

human IPF fibroblasts respond to enhanced expression of these fibrosis resolution genes, with decreased expression of profibrotic genes as well as reduced matrix synthesis and contraction (Figure 6G).

Discussion

Fibroblasts are the key driver of excess ECM deposition in pulmonary fibrosis. Advances in single-cell approaches are beginning to unravel the heterogeneity in lung fibroblasts that are present in health and disease (45–48). A common theme emerging from fibroblast single-cell RNA-seq analyses from experimental models of lung fibrosis is that a variety of fibroblast subsets is capable of contributing to ECM synthesis (44, 49). Hence, in this article, we focused on a deep analysis of the transcriptional changes observed across the entire population of collagen-expressing fibroblasts, identified as Col1α1-GFP positive and CD31/CD45/CD326 negative. Understanding the drivers of the changes in the behavior of this cell population may provide novel avenues for arresting or reversing pulmonary fibrosis. In particular, we focused our analysis on the changes in fibroblast gene signatures as the lung transitions from peak ECM deposition (D14) to an early stage of fibrosis resolution (D30) (3). Fibroblasts isolated at these time points showed a robust activation and reversion at the population level. Interestingly, we observed that fibroblast activation after bleomycin injury was accompanied by both pronounced increases and decreases in gene expression, consistent with prior work showing that repression of gene expression is an essential step in functional fibroblast activation (3, 50). Strikingly, we observed a robust reversal of these alterations in gene expression by D30 after bleomycin, indicating the degree to which fibroblast activation after bleomycin is a transient and largely reversible process. We believe these data provide an important resource for identifying the pathways and regulators that control this reversible switch in fibroblast cell state. In particular, studies of genes and pathways that are repressed during fibrosis and elevated during fibrosis resolution may identify key factors that are capable of reversing fibroblast activation.

As an initial foray into hypothesis testing, we selected two genes identified by our unbiased analyses for further testing. CRISPR-mediated activation to enhance the endogenous expression of either *ALDH2* or *NR3C1* was sufficient to reduce expression of profibrotic gene expression as well as matrix deposition and contraction in IPF fibroblasts. These studies demonstrate the value of our population-level analysis of fibrosis resolution genes in mice and their potential utility in identifying novel approaches for arresting or reversing

pathological fibroblast activation in human cells (Figure 6G). Future study will be necessary to identify the potential mechanisms of action of these genes and their roles in fibrosis resolution, including myofibroblast dedifferentiation, apoptosis, ECM degradation, or antiproliferation responses. Notably, CRISPR activation provides a facile method to rapidly test whether enhancement of endogenous gene expression can beneficially alter profibrotic gene expression and function. The same general approach can also be harnessed to test the inhibition of endogenous gene expression (51) as well as to control specific epigenetic processes that enhance/repress gene expression (52–54). Although not currently feasible for human diseases, harnessing the power of such approaches for therapeutic benefit may become possible in the future, allowing for targeted manipulation of endogenous gene programs *in vivo* (55).

Our study builds on prior work showing that fibrogenic cells undergo dramatic deactivation after transient injury and repair, particularly in the liver (6, 8, 56). Although recent studies have emphasized the role of apoptotic clearance of fibrogenic cells as a mechanism to terminate lung fibrosis (57, 58), our work highlights an accompanying prominent role for deactivation and provides a rich dataset from which to identify potential regulators of this deactivation process. An important limitation of our study is the use of a constitutive Col1α1-GFP reporter for fibroblast isolation. With this approach, we cannot exclude the possibility that populations of newly GFP-expressing cells may emerge in (or depart from) our analyses at each time point, and thus our studies are likely complicated by the entry and exit of cell subgroups into this population. The use of lineage-labeling approaches may provide a powerful alternative for future work, as will the use of more restricted lineage markers of fibroblast subsets as they are identified and validated. However, the ultimate power of these analyses is in hypothesis generation, and our limited work supports the overall utility of our approach in this regard. Further cross-validation of our gene and pathway lists with emerging single-cell and population datasets from human and experimental fibrosis (44–48) may further help to narrow our focus to regulatory pathways that are lacking in human disease. Notably, analysis of a recent single-cell analysis of IPF lungs (44) validated the relevance of *ALDH2* and *NR3C1*. Similarly, analysis of fibroblasts in nonresolving fibrosis models, for example, in the aging mouse (29, 59), may help to identify the differential gene programs that mediate reversal versus sustained activation of fibrogenic cell activation. In summary, the combination of population-level analyses of freshly sorted fibroblasts and hypothesis testing in cultured IPF fibroblasts developed here offers a valuable path toward the identification of novel regulators of lung fibroblast deactivation with potential relevance to understanding fibrosis resolution and its failure in human disease conditions. ■

Author disclosures are available with the text of this article at www.atsjournals.org.

Acknowledgment: The authors thank Dr. Derek Radisky for kindly providing Col1α1-GFP transgenic mice and Mrunal Dehankar for supporting bioinformatics analysis. They also thank Dr. Peter Bitterman and Dr. Craig Henke at the University of Minnesota for providing human lung fibroblasts.

References

1. Betensley A, Sharif R, Karamichos D. A systematic review of the role of dysfunctional wound healing in the pathogenesis and treatment of idiopathic pulmonary fibrosis. *J Clin Med* 2016;6:2.
2. Moeller A, Ask K, Warburton D, Gauldie J, Kolb M. The bleomycin animal model: a useful tool to investigate treatment options for idiopathic pulmonary fibrosis? *Int J Biochem Cell Biol* 2008;40:362–382.
3. Caporarello N, Meridew JA, Jones DL, Tan Q, Haak AJ, Choi KM, *et al*. PGC1α repression in IPF fibroblasts drives a pathologic metabolic, secretory and fibrogenic state. *Thorax* 2019;74:749–760.
4. El Agha E, Moiseenko A, Kheirollahi V, De Langhe S, Crnkovic S, Kwapiszewska G, *et al*. Two-way conversion between lipogenic and myogenic fibroblastic phenotypes marks the progression and resolution of lung fibrosis. *Cell Stem Cell* 2017;20:261–273, e3.
5. Glasser SW, Hagood JS, Wong S, Taype CA, Madala SK, Hardie WD. Mechanisms of lung fibrosis resolution. *Am J Pathol* 2016;186: 1066–1077.
6. Liu X, Xu J, Brenner DA, Kisseleva T. Reversibility of liver fibrosis and inactivation of fibrogenic myofibroblasts. *Curr Pathobiol Rep* 2013;1: 209–214.
7. Kisseleva T, Cong M, Paik Y, Scholten D, Jiang C, Benner C, *et al*. Myofibroblasts revert to an inactive phenotype during regression of liver fibrosis. *Proc Natl Acad Sci USA* 2012;109:9448–9453.
8. Liu X, Xu J, Rosenthal S, Zhang LJ, McCubbin R, Meshgin N, *et al*. Identification of lineage-specific transcription factors that prevent activation of hepatic stellate cells and promote fibrosis resolution. *Gastroenterology* 2020;158:1728–1744, e14.
9. Yata Y, Scanga A, Gillan A, Yang L, Reif S, Breindl M, *et al*. DNase I-hypersensitive sites enhance alpha1(I) collagen gene expression in hepatic stellate cells. *Hepatology* 2003;37:267–276.
10. Tan Q, Ma XY, Liu W, Meridew JA, Jones DL, Haak AJ, *et al*. Nascent lung organoids reveal epithelium- and bone morphogenetic protein-mediated suppression of fibroblast activation. *Am J Respir Cell Mol Biol* 2019;61:607–619.
11. Liu W, Meridew JA, Aravamudhan A, Ligresti G, Tschumperlin DJ, Tan Q. Targeted regulation of fibroblast state by CRISPR-mediated CEBPA expression. *Respir Res* 2019;20:281.
12. Lama V, Moore BB, Christensen P, Toews GB, Peters-Golden M. Prostaglandin E2 synthesis and suppression of fibroblast proliferation by alveolar epithelial cells is cyclooxygenase-2-dependent. *Am J Respir Cell Mol Biol* 2002;27:752–758.
13. Lakatos HF, Thatcher TH, Kottmann RM, Garcia TM, Phipps RP, Sime PJ. The role of PPARs in lung fibrosis. *PPAR Res* 2007;2007:71323.
14. Onozuka I, Kakinuma S, Kamiya A, Miyoshi M, Sakamoto N, Kiyohashi K, *et al*. Cholestatic liver fibrosis and toxin-induced fibrosis are exacerbated in matrix metalloproteinase-2 deficient mice. *Biochem Biophys Res Commun* 2011;406:134–140.
15. Baghy K, Dezso K, László V, Fullár A, Péterfia B, Paku S, *et al*. Ablation of the decorin gene enhances experimental hepatic fibrosis and impairs hepatic healing in mice. *Lab Invest* 2011;91:439–451.
16. Buckley CD, Filer A, Haworth O, Parsonage G, Salmon M. Defining a role for fibroblasts in the persistence of chronic inflammatory joint disease. *Ann Rheum Dis* 2004;63:ii92–ii95.
17. Hartupee J, Mann DL. Role of inflammatory cells in fibroblast activation. *J Mol Cell Cardiol* 2016;93:143–148.
18. Croft AP, Campos J, Jansen K, Turner JD, Marshall J, Attar M, *et al*. Distinct fibroblast subsets drive inflammation and damage in arthritis. *Nature* 2019;570:246–251.
19. Al-Tamari HM, Dabral S, Schmall A, Sarvari P, Ruppert C, Paik J, *et al*. FoxO3 an important player in fibrogenesis and therapeutic target for idiopathic pulmonary fibrosis. *EMBO Mol Med* 2018;10:276–293.

20. Nakagome K, Dohi M, Okunishi K, Tanaka R, Miyazaki J, Yamamoto K. *In vivo* IL-10 gene delivery attenuates bleomycin induced pulmonary fibrosis by inhibiting the production and activation of TGF-beta in the lung. *Thorax* 2006;61:886–894.
21. Steen EH, Wang X, Balaji S, Butte MJ, Bollyky PL, Keswani SG. The role of the anti-inflammatory cytokine interleukin-10 in tissue fibrosis. *Adv Wound Care (New Rochelle)* 2020;9:184–198.
22. Marchitti SA, Brocker C, Stagos D, Vasiliou V. Non-P450 aldehyde oxidizing enzymes: the aldehyde dehydrogenase superfamily. *Expert Opin Drug Metab Toxicol* 2008;4:697–720.
23. Ohta S, Ohsawa I, Kamino K, Ando F, Shimokata H. Mitochondrial ALDH2 deficiency as an oxidative stress. *Ann N Y Acad Sci* 2004; 1011:36–44.
24. Wenzel P, Müller J, Zurmeyer S, Schuhmacher S, Schulz E, Oelze M, *et al*. ALDH-2 deficiency increases cardiovascular oxidative stress: evidence for indirect antioxidative properties. *Biochem Biophys Res Commun* 2008;367:137–143.
25. Juarez MM, Chan AL, Norris AG, Morrissey BM, Albertson TE. Acute exacerbation of idiopathic pulmonary fibrosis-a review of current and novel pharmacotherapies. *J Thorac Dis* 2015;7:499–519.
26. Ma D, Peng L. Vitamin D and pulmonary fibrosis: a review of molecular mechanisms. *Int J Clin Exp Pathol* 2019;12:3171–3178.
27. Wu M, Melichian DS, Chang E, Warner-Blankenship M, Ghosh AK, Varga J. Rosiglitazone abrogates bleomycin-induced scleroderma and blocks profibrotic responses through peroxisome proliferator-activated receptor-gamma. *Am J Pathol* 2009;174:519–533.
28. Marra F, DeFranco R, Robino G, Novo E, Efsen E, Pastacaldi S, *et al*. Thiazolidinedione treatment inhibits bile duct proliferation and fibrosis in a rat model of chronic cholestasis. *World J Gastroenterol* 2005;11:4931–4938.
29. Hecker L, Logsdon NJ, Kurundkar D, Kurundkar A, Bernard K, Hock T, *et al*. Reversal of persistent fibrosis in aging by targeting Nox4-Nrf2 redox imbalance. *Sci Transl Med* 2014;6:231ra47.
30. Patsenker E, Schneider V, Ledermann M, Saegesser H, Dorn C, Hellerbrand C, *et al*. Potent antifibrotic activity of mTOR inhibitors sirolimus and everolimus but not of cyclosporine A and tacrolimus in experimental liver fibrosis. *J Hepatol* 2011;55:388–398.
31. Rehman M, Vodret S, Braga L, Guarnaccia C, Celsi F, Rossetti G, *et al*. High-throughput screening discovers antifibrotic properties of haloperidol by hindering myofibroblast activation. *JCI Insight* 2019;4: e123987.
32. Li S, Wang Y, Chen L, Wang Z, Liu G, Zuo B, *et al*. Beraprost sodium mitigates renal interstitial fibrosis through repairing renal microvessels. *J Mol Med (Berl)* 2019;97:777–791.
33. Hasegawa Y, Ikeda K, Chen Y, Alba DL, Stifler D, Shinoda K, *et al*. Repression of adipose tissue fibrosis through a PRDM16-GTF2IRD1 complex improves systemic glucose homeostasis. *Cell Metab* 2018; 27:180–194, e6.
34. Rajakumari S, Wu J, Ishibashi J, Lim HW, Giang AH, Won KJ, *et al*. EBF2 determines and maintains brown adipocyte identity. *Cell Metab* 2013;17:562–574.
35. Zerr P, Palumbo-Zerr K, Huang J, Tomcik M, Sumova B, Distler O, *et al*. Sirt1 regulates canonical TGF-β signalling to control fibroblast activation and tissue fibrosis. *Ann Rheum Dis* 2016;75:226–233.
36. Zeng Z, Cheng S, Chen H, Li Q, Hu Y, Wang Q, *et al*. Activation and overexpression of Sirt1 attenuates lung fibrosis via P300. *Biochem Biophys Res Commun* 2017;486:1021–1026.
37. Pandit KV, Corcoran D, Yousef H, Yarlagadda M, Tzouvelekis A, Gibson KF, *et al*. Inhibition and role of let-7d in idiopathic pulmonary fibrosis. *Am J Respir Crit Care Med* 2010;182:220–229.
38. Bauman KA, Wettlaufer SH, Okunishi K, Vannella KM, Stoolman JS, Huang SK, *et al*. The antifibrotic effects of plasminogen activation occur via prostaglandin E2 synthesis in humans and mice. *J Clin Invest* 2010;120:1950–1960.
39. Lu NZ, Cidlowski JA. Translational regulatory mechanisms generate N-terminal glucocorticoid receptor isoforms with unique transcriptional target genes. *Mol Cell* 2005;18:331–342.
40. Roos AB, Nord M. The emerging role of C/EBPs in glucocorticoid signaling: lessons from the lung. *J Endocrinol* 2012;212:291–305.
41. Miller M, Cho JY, McElwain K, McElwain S, Shim JY, Manni M, *et al*. Corticosteroids prevent myofibroblast accumulation and airway remodeling in mice. *Am J Physiol Lung Cell Mol Physiol* 2006;290: L162–L169.
42. Lederer DJ, Martinez FJ. Idiopathic pulmonary fibrosis. *N Engl J Med* 2018;378:1811–1823.
43. Richeldi L, Davies HR, Ferrara G, Franco F. Corticosteroids for idiopathic pulmonary fibrosis. *Cochrane Database Syst Rev* 2003;(3): CD002880.
44. Tsukui T, Sun KH, Wetter JB, Wilson-Kanamori JR, Hazelwood LA, Henderson NC, *et al*. Collagen-producing lung cell atlas identifies multiple subsets with distinct localization and relevance to fibrosis. *Nat Commun* 2020;11:1920.
45. Reyfman PA, Walter JM, Joshi N, Anekalla KR, McQuattie-Pimentel AC, Chiu S, *et al*. Single-cell transcriptomic analysis of human lung provides insights into the pathobiology of pulmonary fibrosis. *Am J Respir Crit Care Med* 2019;199:1517–1536.
46. Morse C, Tabib T, Sembrat J, Buschur KL, Bittar HT, Valenzi E, *et al*. Proliferating SPP1/MERTK-expressing macrophages in idiopathic pulmonary fibrosis. *Eur Respir J* 2019;54:1802441.
47. Adams TS, Schupp JC, Poli S, Ayaub EA, Neumark N, Ahangari F, *et al*. Single-cell RNA-seq reveals ectopic and aberrant lung-resident cell populations in idiopathic pulmonary fibrosis. *Sci Adv* 2020;6: eaba1983.
48. Habermann AC, Gutierrez AJ, Bui LT, Yahn SL, Winters NI, Calvi CL, *et al*. Single-cell RNA sequencing reveals profibrotic roles of distinct epithelial and mesenchymal lineages in pulmonary fibrosis. *Sci Adv* 2020;6:eaba1972.
49. Liu X, Rowan SC, Liang J, Yao C, Huang G, Deng N, *et al*. Definition and signatures of lung fibroblast populations in development and fibrosis in mice and men [preprint]. bioRxiv; 2020 [accessed 2020 Jul 15]. Available from: https://www.biorxiv.org/content/10.1101/2020.07.15.203141v1.
50. Jones DL, Meridew JA, Ducharme MT, Lydon KL, Choi KM, Caporarello N, *et al*. ZNF416 is a pivotal transcriptional regulator of fibroblast mechano-activation [preprint]. bioRxiv; 2020 [accessed 2020 Jul 23]. Available from: https://www.biorxiv.org/content/10.1101/2020.07.23.218842v1.
51. Qi LS, Larson MH, Gilbert LA, Doudna JA, Weissman JS, Arkin AP, *et al*. Repurposing CRISPR as an RNA-guided platform for sequence-specific control of gene expression. *Cell* 2013;152:1173–1183.
52. Tan Q, Tschumperlin DJ. Epigenome editing enters the arena: a new tool to reveal (and reverse?) pathologic gene regulation. *Am J Respir Crit Care Med* 2018;198:549–551.
53. Qu J, Zhu L, Zhou Z, Chen P, Liu S, Locy ML, *et al*. Reversing mechanoinductive DSP expression by CRISPR/dCas9-mediated epigenome editing. *Am J Respir Crit Care Med* 2018;198:599–609.
54. Pulecio J, Verma N, Mejía-Ramírez E, Huangfu D, Raya A. CRISPR/Cas9-based engineering of the epigenome. *Cell Stem Cell* 2017;21:431–447.
55. Hirakawa MP, Krishnakumar R, Timlin JA, Carney JP, Butler KS. Gene editing and CRISPR in the clinic: current and future perspectives. *Biosci Rep* 2020;40:BSR20200127.
56. Ramachandran P, Iredale JP, Fallowfield JA. Resolution of liver fibrosis: basic mechanisms and clinical relevance. *Semin Liver Dis* 2015;35: 119–131.
57. Schafer MJ, White TA, Iijima K, Haak AJ, Ligresti G, Atkinson EJ, *et al*. Cellular senescence mediates fibrotic pulmonary disease. *Nat Commun* 2017;8:14532.
58. Baker DJ, Wijshake T, Tchkonia T, LeBrasseur NK, Childs BG, van de Sluis B, *et al*. Clearance of p16Ink4a-positive senescent cells delays ageing-associated disorders. *Nature* 2011;479:232–236.
59. Caporarello N, Meridew JA, Aravamudhan A, Jones DL, Austin SA, Pham TX, *et al*. Vascular dysfunction in aged mice contributes to persistent lung fibrosis. *Aging Cell* 2020;19:e13196.